RAPID COMMUNICATIONS

PHYSICAL REVIEW E **71**, 045301(R) (2005)

Two-fluid model based on the lattice Boltzmann equation

Tiefeng Wang and Jinfu Wang*

Beijing Key Laboratory of Green Reaction Engineering and Technology, Department of Chemical Engineering, Tsinghua University, Beijing 100084, People's Republic of China

(Received 13 January 2005; published 28 April 2005)

A two-fluid model for dispersed two-phase flows based on the lattice Boltzmann equation (LBE) is proposed. Two sets of LBEs are used to describe the two phases. The continuity and Navier-Stokes equations for the continuum-based two-fluid model are obtained from the LBEs by adding a pressure term. The phase holdup is readily calculated from the partial pressure of each phase because the two phases are described by the ideal gas equation of state. A simulated laminar gas-liquid two-phase flow gave good agreement with the results calculated by the conventional continuum-based two-fluid model.

DOI: 10.1103/PhysRevE.71.045301 PACS number(s): 47.55.Kf, 47.11.+j, 05.20.Dd

Two-phase flows are widely used in many industrial processes, and computational fluid dynamics (CFD) simulations of two-phase flows are useful for both practical and academic interests. CFD approaches for two-phase flows generally fall into two categories, namely the Euler-Euler approach [1–4] and the Euler-Lagrange approach [5,6]. The Euler-Euler approach, also called the two-fluid model, has much lower computational demands and is the only practical method for simulating large-scale systems. All the two-fluid models reported in the literature are based on the Navier-Stokes equations. In the last decade, the lattice Boltzmann model (LBM) has been rapidly developed as an attractive method for computational fluid dynamics [7–12]. The implementation of a LBM procedure is much easier than that of continuum-based CFD methods. Parallelization of the LBM is natural since the relaxation is local and the communication pattern in propagation is one way, and the performance increases nearly linearly with the number of CPUs. The pressure can be usually derived from a simple equation of state, instead of solving a Poisson or a Poisson-like equation. Recently, Chen *et al.* [13] showed that the LBM coupled with a turbulence model is likely to offer significant advantages over the conventional continuum-based model. Due to these advantages, the LBM has been successfully used to simulate many problems, including multiphase flows and multicomponent flows [14–19].

Házi *et al.* [20] have reviewed multiphase models based on the lattice Boltzmann equation (LBE). Typical LBE-based multiphase models are the color model [14], the pseudopotential model [15,16], and the free-energy model [17]. All these models focus on the details of flow at the level of individual bubbles or droplets and cannot be used to simulate large-scale systems such as a chemical reactor. In this paper, we propose a LBE-based two-fluid model by adding a modification term to the pressure gradient in the LBE, and validate this model by comparing it with the continuum-based two-fluid model.

The underlying assumption of a continuum approach is that a medium may be divided indefinitely without losing any of its defining properties. Even though each phase in a gas-liquid or liquid-liquid two-phase flow is intrinsically discrete, various averaging techniques can be applied to describe it by a continuum model. The equations that govern the dynamics of a two-phase flow have been well discussed in the literature [1–4]. They are two sets of mass and momentum conservation equations for an isothermal flow. Here we take a gas-liquid flow without an interfacial mass transfer as an example for illustration. The dimensionless form of the continuum-based two-fluid model for the isothermal gas-liquid flow is as follows:

$$\frac{\partial}{\partial \hat{t}}(\alpha_k \hat{\rho}_k) + \nabla_{\hat{x}} \cdot (\alpha_k \hat{\rho}_k \hat{\mathbf{v}}_k) = 0, \tag{1}$$

$$\frac{\partial}{\partial \hat{t}}(\alpha_k \hat{\rho}_k \hat{\mathbf{v}}_k) + \nabla_{\hat{x}} \cdot (\alpha_k \hat{\rho}_k \hat{\mathbf{v}}_k \hat{\mathbf{v}}_k) = -\alpha_k \nabla_{\hat{x}} \hat{p} + \hat{\nu}_k \nabla \cdot [\hat{\alpha}_k \hat{\rho}_k (\nabla_{\hat{x}} \hat{\mathbf{v}}_k + (\nabla_{\hat{x}} \hat{\mathbf{v}}_k)^T)] + \hat{\mathbf{F}}_k, \tag{2}$$

where the subscript k is l and g, for the continuous liquid and dispersed gas phase, respectively. α_l and α_g are the liquid and gas holdups, and satisfy the constraint $\alpha_l + \alpha_g = 1$. The force term $\mathbf{F}_k$ includes the body force, e.g., gravity force, and the interphase forces.

The lattice Boltzmann equation with the Bhatnagar-Gross-Krook (BGK) [21] approximation can be expressed as

$$f_i(\mathbf{x} + \mathbf{e}_i \Delta t, t + \Delta t) - f_i(\mathbf{x}, t) = -\frac{1}{\tau}[f_i(\mathbf{x}, t) - f_i^{(eq)}(\mathbf{x}, t)] + \Delta t F_i, \tag{3}$$

where $f_i(\mathbf{x}, t)$ is the distribution function for particles with velocity $\mathbf{e}_i$ at position $\mathbf{x}$ and time t, and Δt is the time increment. $f_i^{(eq)}$ is the equilibrium distribution function, and τ is the dimensionless relaxation time.

For simplicity and without losing generality, we use the 2-D-9-velocity (D2Q9) model [22] to develop the LBE-based two-fluid model. In the D2Q9 model, the particle velocities are defined by $\mathbf{e}_0 = (0,0)$, $\mathbf{e}_i = (\cos[\pi(i-1)/2], \sin[\pi(i-1)/2])c$ for $i = 1-4$ and $\mathbf{e}_i = (\cos[\pi(i$

*Author to whom correspondence should be addressed. FAX: +86-10-62772051. Email address: wangjf@flotu.org

$-9/2)/2], \sin[\pi(i-9/2)/2])c$ for $i=5-8$. Here $c=\Delta x/\Delta t$, and Δx is the lattice spacing. We consider the following two sets of LBEs with the same time increment Δt and lattice spacing Δx for the two phases

$$f_{k,i}(\mathbf{x}+\mathbf{e}_i\Delta t, t+\Delta t) - f_{k,i}(\mathbf{x},t) = -\frac{1}{\tau_k}[f_{k,i}(\mathbf{x},t) - f_{k,i}^{(eq)}(\mathbf{x},t)] + \Delta t F_{k,i} \quad k=l,g, \tag{4}$$

where the force term $F_{k,i}$ is calculated by the method proposed by Guo *et al.* [23]

$$f_{k,i}^{(eq)} = w_i\rho_k\left\{1+\frac{3(\mathbf{e}_i\cdot\mathbf{u}_k)}{c^2}+\frac{9(\mathbf{e}_i\cdot\mathbf{u}_k)^2}{2c^4}+\frac{3\ \mathbf{u}_k{}^2)}{2c^2}\right\}, \tag{5}$$

$$\mathbf{u}_k = \frac{1}{\rho_k}\left(\sum_i \mathbf{e}_i f_{k,i} + \frac{1}{2}\mathbf{F}_k\Delta t\right), \tag{6}$$

$$F_{k,i} = \left(1-\frac{1}{2\tau_k}\right)w_i\left(\frac{3(\mathbf{e}_i-\mathbf{u}_k)}{c^2}+\frac{9(\mathbf{e}_i\cdot\mathbf{u}_k)}{c^4}\mathbf{e}_i\right)\cdot\mathbf{F}_k, \tag{7}$$

where the weights $w_0=4/9$, $w_i=1/9$ for $i=1-4$, and $w_i=1/36$ for $i=5-8$.

The fluid density ρ_k and velocity $\mathbf{u}_k$ are determined by the distribution function $f_{k,i}(\mathbf{x},t)$ and the force term $\mathbf{F}_k$

$$\rho_k = \sum_i f_{k,i}, \tag{8}$$

$$\rho_k\mathbf{u}_k = \sum_i f_{k,i}\mathbf{e}_i + \frac{1}{2}\mathbf{F}_k\Delta t. \tag{9}$$

By defining the dimensionless quantities $\hat{x}=x/\Delta x$, $\hat{t}=t/\Delta t$, $\hat{e}_i=e_i/c$, $\hat{\mathbf{u}}_k=\mathbf{u}_k/c$, $\hat{\rho}_k=\rho_k/\rho_{k,0}$, $\hat{f}_{k,i}=\hat{f}_{k,i}/\rho_{k,0}$, $\hat{F}_{k,i}=F_{k,i}/(\rho_{k,0}c)$, $\hat{\mathbf{F}}_k=\mathbf{F}_k\Delta t/(\rho_{k,0}c)$, we get the dimensionless form of Eqs. (4)–(9)

$$\hat{f}_{k,i}(\hat{\mathbf{x}}+\hat{\mathbf{e}}_i,\hat{t}+1) - \hat{f}_{k,i}(\hat{\mathbf{x}},\hat{t}) = -\frac{1}{\tau_k}[\hat{f}_{k,i}(\hat{\mathbf{x}},\hat{t}) - \hat{f}_{k,i}^{(eq)}(\hat{\mathbf{x}},\hat{t})] + \hat{F}_{k,i}, \tag{10}$$

$$\hat{f}_{k,i}^{(eq)} = w_i\hat{\rho}_k\{1+3(\hat{\mathbf{e}}_i\cdot\hat{\mathbf{u}}_k)+\tfrac{9}{2}(\hat{\mathbf{e}}_i\cdot\hat{\mathbf{u}}_k)^2+\tfrac{3}{2}\hat{\mathbf{u}}_k\}, \tag{11}$$

$$\hat{\mathbf{u}}_k = \frac{1}{\hat{\rho}_k}\left(\sum_i \hat{\mathbf{e}}_i\hat{f}_{k,i}+\frac{\hat{\mathbf{F}}_k}{2}\right), \tag{12}$$

$$\hat{F}_{k,i} = \left(1-\frac{1}{2\tau_k}\right)w_i[3(\hat{\mathbf{e}}_i-\hat{\mathbf{u}}_k)+9(\hat{\mathbf{e}}_i\cdot\hat{\mathbf{u}}_k)\hat{\mathbf{e}}_i]\cdot\hat{\mathbf{F}}_k, \tag{13}$$

$$\hat{\rho}_k = \sum_i \hat{f}_{k,i}, \tag{14}$$

$$\hat{\rho}_k\hat{\mathbf{u}}_k = \sum_i \hat{f}_{k,i}\hat{\mathbf{e}}_i + \tfrac{1}{2}\hat{\mathbf{F}}_k. \tag{15}$$

By the Chapman-Enskog expansion [23,24], Eq. (10) leads to the following continuity equation and Navier-Stokes equation:

$$\frac{\partial\hat{\rho}_k}{\partial\hat{t}} + \nabla_{\hat{x}}\cdot(\hat{\rho}_k\hat{\mathbf{u}}_k) = 0, \tag{16}$$

$$\frac{\partial}{\partial\hat{t}}(\hat{\rho}_k\hat{\mathbf{u}}_k) + \nabla_{\hat{x}}\cdot(\hat{\rho}_k\hat{\mathbf{u}}_k\hat{\mathbf{u}}_k) = -\nabla_{\hat{x}}\hat{p}_k + \hat{\nu}_k\nabla_{\hat{x}}\cdot\{\hat{\rho}_k[\nabla_{\hat{x}}\hat{\mathbf{u}}_k + (\nabla_{\hat{x}}\hat{\mathbf{u}}_k)^T]\} + \hat{\mathbf{F}}_k. \tag{17}$$

Defining $\hat{\rho}_T=\hat{\rho}_g+\hat{\rho}_l$, $\alpha_k=\hat{\rho}_k/\hat{\rho}_T$, $\hat{p}_k=p_k/(\rho_{k,0}c^2)$, $\hat{p}_T=\hat{p}_g+\hat{p}_l$, we have $\hat{p}_k=\frac{1}{3}\hat{\rho}_k$ and $\alpha_k=\hat{p}_k/\hat{p}_T$. Equations (16) and (17) can be also expressed as

$$\frac{\partial\alpha_k\hat{\rho}_T}{\partial\hat{t}} + \nabla_{\hat{x}}\cdot(\alpha_k\hat{\rho}_T\hat{\mathbf{u}}_k) = 0, \tag{18}$$

$$\frac{\partial}{\partial\hat{t}}(\alpha_k\hat{\rho}_T\hat{\mathbf{u}}_k) + \nabla_{\hat{x}}\cdot(\alpha_k\hat{\rho}_T\hat{\mathbf{u}}_k\hat{\mathbf{u}}_k) = -\nabla_{\hat{x}}(\alpha_k\hat{p}_T) + \hat{\nu}_k\nabla_{\hat{x}}\cdot[\alpha_k\hat{\rho}_T[\nabla_{\hat{x}}\hat{\mathbf{u}} + (\nabla_{\hat{x}}\hat{\mathbf{u}}_k)^T]] + \hat{\mathbf{F}}_k. \tag{19}$$

If we set $\hat{\rho}_k$ in Eqs. (1) and (2) to be $\hat{\rho}_T$ in Eqs. (18) and (19), then Eq. (18) is the same as Eq. (1), and the only difference between Eqs. (19) and (2) is the pressure gradient term, which is $-\alpha_k\nabla_{\hat{x}}(\hat{p}_k)$ in Eq. (2) and $-\nabla_{\hat{x}}(\alpha_k\hat{p}_T)$ in Eq. (19). Since $\nabla_{\hat{x}}(\alpha_k\hat{p}_T)=\alpha_k\nabla_{\hat{x}}(\hat{p}_T)+\hat{p}_T\nabla_{\hat{x}}(\alpha_k)$, the two-fluid model can be recovered from the LBE with approximation to the second order by adding a force term $\hat{p}_T\nabla_{\hat{x}}(\alpha_k)$ to the right-hand side of Eq. (19). The final LBE for the two-fluid model is

$$\hat{f}_{k,i}(\hat{\mathbf{x}}+\hat{\mathbf{e}}_i,\hat{t}+1) - \hat{f}_{k,i}(\hat{\mathbf{x}},\hat{t}) = -\frac{1}{\tau_k}[\hat{f}_{k,i}(\hat{\mathbf{x}},\hat{t}) - \hat{f}_{k,i}^{(eq)}(\hat{\mathbf{x}},\hat{t})] + \hat{p}_T\nabla_{\hat{x},i}(\alpha_k) + \hat{F}_{k,i} \tag{20}$$

where $\hat{f}_{k,i}^{(eq)}$ and $\hat{F}_{k,i})$ are the same as in Eqs. (11)–(13).

Thus, we have constructed a LBE-based two-fluid model for large-scale two-phase flows. The treatment of the force term in Eq. (20) needs some further discussion. In a gas-liquid flow, the forces on the gas phase include the virtual mass force $\mathbf{F}_{g,VM}$, gravity force $\mathbf{F}_{g,G}$, buoyancy force $\mathbf{F}_{g,BU}$, drag force $\mathbf{F}_{g,DR}$, lift force $\mathbf{F}_{g,L}$, and dispersion force $\mathbf{F}_{g,DP}$ [4]. The virtual mass force $\mathbf{F}_{g,VM}$ describes the physics that a part of a liquid near a bubble is accelerated together with the bubble [25]. The lift force $\mathbf{F}_{g,L}$ is induced by the interaction between the bubble and liquid shear flow [26]. The dispersion force $\mathbf{F}_{g,DP}$ in a laminar bubbly flow is caused by bubble fluctuating motion due to deformation, and has a larger value for bubbles of larger size [27]. These interface forces are expressed as

$$\mathbf{F}_{g,VM} = \alpha_g\rho_l C_{VM}\frac{\mathrm{D}}{\mathrm{D}t}(\mathbf{u}_g-\mathbf{u}_l), \tag{21}$$

$$\mathbf{F}_{g,G} = \alpha_g\rho_g\mathbf{g}, \tag{22}$$

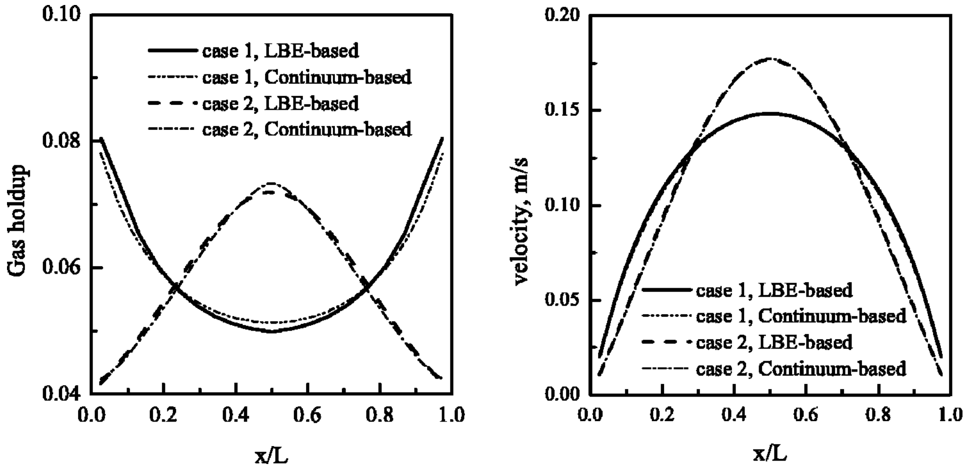

FIG. 1. Comparison between the continuum-based and LBE-based two-fluid models. $U_l=0.1$ m/s, $U_g=0.012$ m/s. x/L is the dimensionless lateral position. Case 1: $C_L=0.05$, $C_{DP}=0.0015$ m^2/s^2. Case 2: $C_L=-0.1$, $C_{DP}=0.003$ m^2/s^2.

$$\mathbf{F}_{g,BU}(\mathbf{x},t)=\alpha_g\rho_l\mathbf{g}, \tag{23}$$

$$\mathbf{F}_{g,DR}=\alpha_g\rho_l\frac{3C_D}{4d_b}(\mathbf{u}_g-\mathbf{u}_l)|\mathbf{u}_g-\mathbf{u}_l|, \tag{24}$$

$$\mathbf{F}_{g,L}=-C_L\alpha_g\rho_l(\mathbf{u}_g-\mathbf{u}_l)\times\nabla\times\mathbf{u}_l, \tag{25}$$

$$\mathbf{F}_{g,DP}=-C_{DP}\rho_l\nabla\alpha_g. \tag{26}$$

The total force on the gas phase is zero, that is,

$$\mathbf{F}_{g,VM}+\mathbf{F}_{g,G}+\mathbf{F}_{g,BU}+\mathbf{F}_{g,DR}+\mathbf{F}_{g,L}+\mathbf{F}_{g,DP}=0. \tag{27}$$

After the liquid phase velocity is determined, the velocity of the gas phase can be determined from Eq. (27). The distribution function $f_{g,i}$ is then obtained by changing the post-propagated distribution to get the desired velocity, that is, set the force term in the LBE of the gas phase as

$$\hat{F}_{g,i}=\begin{cases}0 & i=0\\ \frac{1}{3}\hat{\rho}_g\hat{\mathbf{e}}_i\cdot(\hat{\mathbf{u}}_{g,bl}-\hat{\mathbf{u}}_g) & i=1-4\\ \frac{1}{12}\hat{\rho}_g\hat{\mathbf{e}}_i\cdot(\hat{\mathbf{u}}_{g,bl}-\hat{\mathbf{u}}_g) & i=5-8,\end{cases} \tag{28}$$

where $\hat{\mathbf{u}}_{g,bl}$ is the dimensionless gas velocity that satisfies the force balance of Eq. (27) and $\hat{\mathbf{u}}_g$ is the dimensionless gas velocity after the propagation step.

For the liquid phase, the force term is much simpler. As discussed above, the total force, including the virtual mass force, buoyancy force, drag force, lift force, and dispersion force, exerted by the liquid phase on the gas phase balances the gravity force of the gas phase. Because the gas density is negligible compared with that of the liquid, the total force exerted by the liquid phase on the gas phase is approximately zero. According to Newton's third law, the total force exerted by the gas phase on the liquid phase is also zero. So the main force on the liquid phase is the buoyancy force that is caused by a nonuniform profile of the gas holdup. This can be calculated in a straightforward manner based on the density variation, which is due to the profile of the gas holdup

$$\hat{\mathbf{F}}_{l,BU}(\mathbf{x},t)=[\hat{\rho}_l(\mathbf{x},t)-\hat{\rho}_{l,ref}(\mathbf{x},t)]\hat{\mathbf{g}}, \tag{29}$$

where $\hat{\rho}_l(\hat{\mathbf{x}},t)$ is calculated by Eq. (14), and $\hat{\mathbf{g}}=\mathbf{g}\Delta t^2/\Delta x$. The buoyancy force that needs to be in the LBE of the liquid phase is calculated with Eqs. (11)–(13).

To validate the proposed model, we compare the simulations of a two-dimensional laminar gas-liquid bubbly flow of the continuum-based two-fluid model and our LBE-based two-fluid model. The physical properties of the simulated two-phase system are: $\rho_l=1000$ kg/m^3, $\rho_g=1$ kg/m^3, $\nu_l=\nu_g=10^{-3}$ Pa s. The virtual mass force coefficient C_{VM} depends on the bubble shape and is set to be 0.25 in this paper, referring to Cook and Harlow [25]. Actually, the virtual mass force only affects the flow evolution with time and has no influence on the final steady flow behavior. The lift force coefficient C_L and dispersion force coefficient C_{DP} are dependent on the bubble size [26,27]. Tomiyama [26] found that C_L varies in the range from 0.288 to −0.29 for gas-liquid systems with liquid of high viscosity. For small bubbles, the direction of the lift force is towards the lower liquid velocity side, while for large bubbles the direction of the lift forces is opposite. Therefore the lateral profile of the gas holdup, which is determined by the lateral forces, is different for bubbles of different sizes. To simulate the different profiles, two sets of parameters are used according to [26,27]: Case 1 is for small bubbles with $C_L=0.05$ and $C_{DP}=0.0015$ m^2/s^2; case 2 is for relatively larger bubbles with $C_L=-0.1$ and $C_{DP}=0.003$ m^2/s^2. For the purpose of comparison, the drag force coefficient is set so that the slip velocity is 0.1 m/s in both cases. We compare the hydrodynamic behavior in the fully developed flow region. The computational domain is 0.095 m in width. The inlet and outlet conditions are set to be periodic boundary conditions for the fully developed flow. The continuum-based two-fluid model is solved with the CFD package CFX4.4. In both simulations using the CFX4.4 package and LBM, the number of lattices used is 20 in width with $\Delta x=5$ mm, and the time step $\Delta t=1$ ms. In LBM simulations, τ is set to be 0.62 to accord with the dynamic viscosity.

The gas holdup and liquid velocity are the two most important parameters in the gas-liquid flow. Figure 1 shows the lateral profiles of the gas holdup and liquid velocity. In case

1, for small bubbles, the lift force is towards the wall, so the gas holdup has a smaller value in the center than in the near-wall region. In case 2, for large bubbles, the lift force is towards the center, so the gas holdup has a larger value in the center. Due to the gas-liquid interaction, the nonuniform radial profile of the liquid velocity in case 2 is more remarkable than in case 1. As can be seen in Fig. 1, the results calculated by the LBE-based model are in good agreement with those calculated by the continuum-based model. This verifies the validity of the LBE-based two-fluid model proposed in this paper. The advantages of the LBE-based two-fluid model are remarkable. Besides the common advantages of the LBM, there are several other attractive characteristics: First, the LBE-based model is explicit, and does not need iteration to solve the coupled continuity and momentum equations for the two phases. Second, the phase holdups are naturally solved from the partial pressures in the LBE-based model and need no additional computational cost. Third, there is no need to solve the Poisson equation because the pressure field can be readily solved from a simple equation of state. These characteristics make the LBE-based model much simpler in code development and more efficient in computation. In the testing problem of this work, the LBE-based model takes less than half of the CPU cost of the continuum-based model for the same number of iterations. Further comparison is needed for parallel computation or when a turbulence model is coupled.

Continuum-based models for a gas-liquid flow average over the details of the flow at the level of the individual bubbles. These details affect the overall behavior through phase interaction terms and the effective stress tensors in the final model equations. In recent years, the multiscale method has been an effective approach to study multiphase flow that involves a wide range of temporal and spatial scales [28,29]. Methods such as direct numerical simulation (DNS), LBM, and volume of fluid (VOF) [30] can be used to simulate the details of the flow. Sankaranarayanan *et al.* [18] and van der Hoef *et al.* [29] explored the use of the LBM as a technique to provide closures for the two-fluid model. Using the LBE-based two-fluid model of this paper, the simulations of different scales can be carried out on the same LBM platform.

The authors are grateful to Professor D.Z. Wang for his helpful discussions.

[1] M. Ishii, *Thermo-Fluid Dynamic Theory of Two-Phase Flow* (Eyrolles, Paris, 1975).
[2] D. A. Drew, Annu. Rev. Fluid Mech. **15**, 261 (1983).
[3] R. Krishna, M. I. Urseanu, J. M. van Baten, and J. Ellenberger, Chem. Eng. Sci. **54**, 4903 (1999).
[4] T. F. Wang, J. F. Wang, and Y. Jin (unpublished).
[5] E. Delnoij, F. A. Lammers, J. A. M. Kuipers, and W. P. M. Van Swaaij, Chem. Eng. Sci. **52**, 429 (1997).
[6] A. Sokolichin, G. Eigenberger, A. Lapin, and A. Lübbert, Chem. Eng. Sci. **52**, 611 (1997).
[7] G. R. McNamara and G. Zanetti, Phys. Rev. Lett. **61**, 2332 (1988).
[8] F. Higuera, S. Succi, and R. Benzi, Europhys. Lett. **9**, 345 (1989); F. Higuera and J. Jiménez, *ibid.* **9**, 663 (1989).
[9] R. Benzi, S. Succi, and M. Vergassola, Phys. Rep. **222**, 145 (1992).
[10] S. Succi, *The Lattice Boltzmann Equation for Fluid Dynamics and Beyond* (Clarendon Press, Oxford, 2001).
[11] X. Shan and X. He, Phys. Rev. Lett. **80**, 65 (1998).
[12] S. Chen and G. D. Doolen, Annu. Rev. Fluid Mech. **30**, 329 (1998).
[13] H. D. Chen, S. Kandasamy, S. Orszag, R. Shock, S. Succi, and V. Yakhot, Science **301**, 633 (2003).
[14] A. K. Gunstensen and D. H. Rothman, Europhys. Lett. **18**, 157 (1992).
[15] X. Shan and H. Chen, Phys. Rev. E **47**, 1815 (1993); X. Shan and G. Doolen, J. Stat. Phys. **81**, 379 (1995).
[16] X. He, X. Shan, and G. D. Doolen, Phys. Rev. E **57**, R13 (1998).
[17] M. R. Swift, W. R. Osborn, and J. M. Yeomans, Phys. Rev. Lett. **75**, 830 (1995); M. R. Swift, E. Orlandini, W. R. Osborn, and J. M. Yeomans, Phys. Rev. E **54**, 5041 (1996).
[18] K. Sankaranarayanan and S. Sundaresan, Chem. Eng. Sci. **57**, 3521 (2002).
[19] L.-S. Luo, Phys. Rev. Lett. **81**, 1618 (1998); L.-S. Luo, Phys. Rev. E **62**, 4982 (2000).
[20] G. Házi, A. R. Imre, G. Mayer, and I. Farkas, Ann. Nucl. Energy **29**, 1421 (2002).
[21] P. L. Bhatnagar, E. P. Gross, and M. Krook, Phys. Rev. **94**, 511 (1954).
[22] Y. H. Qian, D. d'Humières, and P. Lallemand, Europhys. Lett. **17**, 479 (1992).
[23] Z. Guo, C. Zheng, and B. Shi, Phys. Rev. E **65**, 046308 (2002).
[24] S. Chapman and T. G. Cowling, *The Mathematical Theory of Non-Uniform Gases*, 3rd ed. (Cambridge University Press, Cambridge, 1970).
[25] T. L. Cook and F. H. Harlow, Int. J. Multiphase Flow **12**, 35 (1986).
[26] A. Tomiyama, Multiphase Sci. Technol. **10**, 369 (1998).
[27] D. Lucas, E. Krepper, and H. M. Prasser, Int. J. Therm. Sci. **40**, 217 (2001).
[28] S. Succi, O. Filippova, G. Smith, and E. Kaxiras, Comput. Sci. Eng. **3**, 26 (2001).
[29] A. van der Hoef, M. van Sint Annaland, and J. A. M. Kuipers, Chem. Eng. Sci. **59**, 5157 (2004).
[30] R. Scardovelli and S. Zaleski, Annu. Rev. Fluid Mech. **31**, 567 (1999).